Lattice thermal conductivity of graphene nanoribbons: Anisotropy and edge roughness scattering

Z. Aksamija[a)] and I. Knezevic[b)]
Department of Electrical and Computer Engineering, University of Wisconsin–Madison, Madison, Wisconsin 53706, USA

We present a calculation of the thermal conductivity of graphene nanoribbons (GNRs), based on solving the Boltzmann transport equation with the full phonon dispersions, a momentum-dependent model for edge roughness scattering, as well as three-phonon and isotope scattering. The interplay between edge roughness scattering and the anisotropy of the phonon dispersions results in thermal conduction that depends on the chiral angle of the nanoribbon. Lowest thermal conductivity occurs in the armchair direction and highest in zig-zag nanoribbons. Both the thermal conductivity and the degree of armchair/zig-zag anisotropy depend strongly on the width of the nanoribbon and the rms height of the edge roughness, with the smallest and most anisotropic thermal conductivities occurring in narrow GNRs with rough edges. © *2011 American Institute of Physics*. [doi:10.1063/1.3569721]

Single-layer graphene is a unique material made up of a monolayer of sp^2-hybridized carbon atoms that is capable of purely two-dimensional electrical[1] and thermal transport.[2] It can be fashioned into a broad range of shapes, from millimeter-sized flakes down to very narrow nanoribbons. Despite single-layer graphene possessing superior thermal conductivity,[3,4] graphene nanoribbons (GNRs) have been shown to have the potential to be excellent thermoelectrics with very high values of the thermoelectric figure-of-merit ZT.[5] The enhancement of ZT has been explained by the fact that the presence of line edge roughness in narrow GNRs affects thermal transport very strongly[6] while leaving electronic transport relatively unchanged.[5] Previous studies of the effect of width, line edge roughness, and anisotropy on thermal conductivity largely relied either on the ballistic approximation[7] or a simplified treatment of edge roughness scattering.[8] Studies based on molecular dynamics also demonstrated the anisotropy of thermal conductivity and sensitivity to width and edge roughness;[9] however, such studies were limited in the range of sizes that could be examined.

In this letter, we study the lattice thermal conductivity in GNRs over a wide range of widths, edge roughness values, and chiral angles. We calculate thermal conductivity by solving the phonon Boltzmann transport equation in the relaxation time approximation, and account for phonon-phonon, phonon-isotope, and edge roughness scattering. We assume a thermal gradient is applied along the nanoribbon and show that thermal conductivity varies with the chiral angle of the ribbon, with a minimum in armchair and a maximum in zig-zag GNRs. The angular variation becomes stronger as the width of the ribbon decreases because of the increased role of phonon scattering with the rough edges of the narrow nanoribbon. Edge roughness scattering also causes the overall value of the thermal conductivity to decrease with decreasing width.

In order to obtain accurate thermal conductivities in an arbitrary transport direction, we employ the full phonon dispersion, shown in Fig. 1. Phonon dispersion has been previously measured by Raman spectroscopy[10] and x-ray scattering[11] and compared to calculations. Based on experimental results, the empirical fourth-nearest-neighbor (4NNR) model of Saito[12] was reparametrized to include new experimental findings[10] and first-principles numerical calculations,[11] while also including off-diagonal terms of the force constant matrices[13] and rotational invariance conditions.[14] The reparametrized 4NNR model has been shown to offer an excellent fit to both experiments and first-principles calculations.[13] We use the 4NNR model with parameters obtained by fitting first-principles results with a small correction to the in- and out-of-plane tangential force constants to satisfy the rotational invariance condition.[14]

Scattering from the rough edges of the nanoribbon is partially diffuse and can be accurately described by a
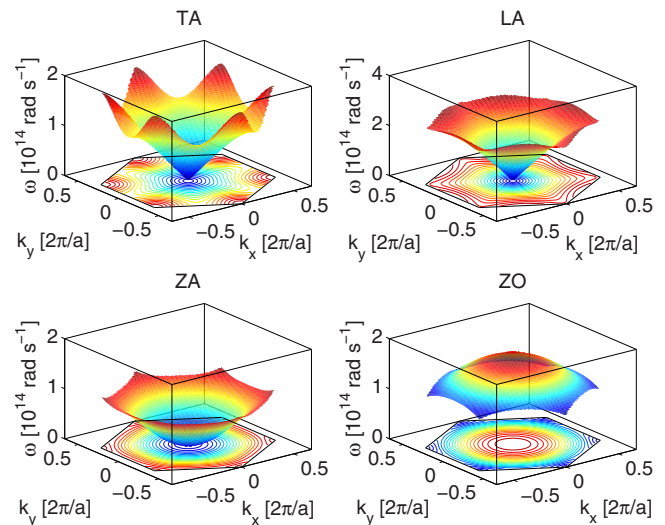
FIG. 1. (Color online) Phonon dispersion relationship of single-layer graphene calculated using the 4NNR model, showing the TA, LA, ZA, and ZO branches over the first Brillouin zone of graphene. The dispersions are strongly anisotropic, causing phonon group velocities (given by the gradients of the radial frequency ω) to be strongly dependent on the direction of the phonon wave vector. The remaining two optical branches (TO and LO) are not depicted due to their negligible contribution to thermal transport.

a)Electronic mail: aksamija@wisc.edu.
b)Electronic mail: knezevic@engr.wisc.edu.

momentum-dependent specularity parameter $0 \le p(\vec{q}) \le 1$, which represents the probability that a phonon mode $\vec{q}$ will be scattered from the rough edge.[15] The lifetime of a phonon with wave vector $\vec{q}$ in branch λ due to the interaction with rough edges is then given by

$$\tau_{\lambda,E}(\vec{q}) = \left[\frac{1+p(\vec{q})}{1-p(\vec{q})}\right]\frac{W}{\upsilon_{\lambda,\perp}(\vec{q})}, \tag{1}$$

where W is the width of the ribbon and $\upsilon_{\lambda,\perp}(\vec{q})$ is the component of the phonon velocity of mode $\vec{q}$ in branch λ perpendicular to the idealized smooth edge of the nanoribbon. The specularity parameter is related to the rms height of edge variations Δ, phonon momentum $\vec{q}$, and angle θ_E between the phonon wave vector and the normal to the nanoribbon edge through[16] $p(\vec{q}) = \exp(-4q^2\Delta^2\cos^2\theta_E)$.

The resistive umklapp phonon-phonon scattering rate can be calculated in the standard general approximation for dielectric crystals[17]

$$\tau_{\lambda,U}^{-1}(\vec{q}) = \frac{\hbar\gamma_\lambda^2}{\bar{M}\Theta_\lambda\bar{v}_\lambda^2}\omega_\lambda^2(\vec{q})Te^{-\Theta_\lambda/3T}, \tag{2}$$

where the speed of sound $\bar{v}_\lambda$ of each branch λ is determined from the average slope of its dispersion curve near the Γ point,[18] and $\bar{M}$ is the average atomic mass. The expression in Eq. (2) has been used successfully for graphene,[18] carbon nanotubes,[19] and GNRs;[8] however, the exponential term $e^{-\Theta_\lambda/3T}$ in the temperature dependence is often omitted. This term controls the onset of resistive umklapp scattering for each phonon branch through the branch-specific Debye temperatures Θ_λ, which were obtained from[20]

$$\Theta_\lambda^2 = \frac{5\hbar^2}{3k_B^2}\frac{\int \omega^2 g_\lambda(\omega)d\omega}{\int g_\lambda(\omega)d\omega}, \tag{3}$$

where the vibrational density of states (vDOS) function $g_\lambda(\omega) = \Sigma_{\vec{q}}\delta[\omega - \omega_\lambda(\vec{q})]$ was calculated for each phonon branch λ from the full dispersion. This way, the temperature dependence of the contribution of each phonon branch to the total thermal conductivity is correctly represented.

The strength of the phonon-phonon scattering process for each branch is controlled by the Grüneissen constant γ_λ, which is deduced from the logarithmic derivative of dispersion with respect to volume $\gamma_\lambda = -[a/2\omega_\lambda(\vec{q})][d\omega_\lambda(\vec{q})/da]$. Based on first-principles calculations for graphene, it was shown that $\gamma_{TA,LA}$ are nearly constant throughout the first Brillouin zone and that the relationship $\gamma_{LA}/\gamma_{TA} \approx 3$ holds for transverse acoustic (TA) and longitudinal acoustic (LA) modes.[18,21] The value of γ_{LA} is generally taken to be 2,[8,18] while the value for out-of-plane acoustic (ZA) and out-of-plane optical (ZO) modes is negative, and can be approximated to be -1.5.[18]

Scattering from mass differences due to the presence of naturally occurring isotopes can be represented by an energy-dependent rate $\tau_I^{-1}(\omega) = \Gamma\Omega_0/12\omega^2 g(\omega)$, with the total vDOS function given by a sum over all branches $g(\omega) = \Sigma_\lambda g_\lambda(\omega)$. The mass-difference constant Γ is given by the sum over all naturally occurring isotopes weighted by their mass M_i relative to the average mass $\bar{M}$,[22] $\Gamma = \Sigma_i f_i(1-M_i/\bar{M})^2 = c(1-c)/(12-c)^2$. Using natural abundances of ^{12}C and ^{13}C of 98.9% and 1.1%, respectively, we obtain $c = 0.011$. Phonon lifetimes due to roughness, phonon-phonon umklapp, and
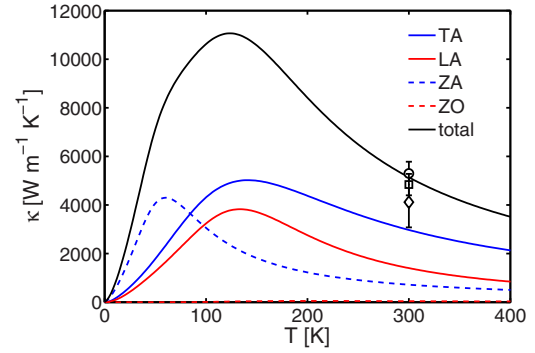
FIG. 2. (Color online) Thermal conductivity results for GNRs of width $W = 5$ μm and rms edge roughness $\Delta = 1$ nm, showing contributions from individual phonon branches (TA, LA, ZA, and ZO) and total. Symbols and error bars are the experimental results for the total thermal conductivity of several suspended nanoribbons, approximately 5 μm wide, taken from Ref. 3 ($\bigcirc$ and $\square$) and Ref. 4 ($\diamond$), shown here for comparison.

isotope scattering are combined according to $\tau_\lambda^{-1}(\vec{q}) = \tau_{\lambda,E}^{-1}(\vec{q}) + \tau_{\lambda,U}^{-1}(\vec{q}) + \tau_I^{-1}[\omega_\lambda(\vec{q})]$ and used to calculate the total thermal conductivity tensor by summing over all the phonon branches $\lambda = TA, LA, ZA, ZO$ that contribute significantly to thermal transport

$$\kappa^{\alpha\beta}(T) = \frac{1}{\delta}\sum_{\lambda,\vec{q}}\upsilon_\lambda^\alpha(\vec{q})\upsilon_\lambda^\beta(\vec{q})\tau_\lambda^{-1}(\vec{q})\hbar\omega_\lambda(\vec{q})\frac{\partial N_0(T)}{\partial T}, \tag{4}$$

with the thickness of the monolayer is assumed to be[23] $\delta = 0.335$ nm, and $\upsilon_\lambda^{\alpha,\beta}(\vec{q})$ is the components of the phonon group velocity vector obtained from the full dispersion by $\upsilon_\lambda^{\alpha,\beta}(\vec{q}) = \partial\omega_\lambda(\vec{q})/\partial\alpha,\beta$.

Figure 2 shows a comparison of the calculated thermal conductivity in a 5 μm wide ribbon with rms edge roughness $\Delta = 1$ nm, indicating excellent agreement with recent measurements on suspended ribbons of that same width.[3,4] In these wide ribbons ($W = 5$ μm), phonon-phonon umklapp scattering dominates at room temperature, as can be seen from the roughly $\kappa \propto 1/T$ behavior in Fig. 2. Since the Grüneissen parameter γ follows $\gamma_{LA}/\gamma_{TA} \approx 3$, the TA mode has the largest contribution to the thermal conductivity at room temperature, while the ZA mode is stronger at low temperatures below the thermal conductivity peak, which occurs around 130 K in the 5 μm wide ribbon.

Angular variation in the lattice thermal conductivity is depicted in Fig. 3. Edge rms roughness Δ is assumed to be 1 nm in all cases.[6] The angle θ_C is taken with respect to the armchair edge of the nanoribbon, so that an angle of zero degrees represents an armchair GNR, while an angle of 30 degrees represents a zig-zag ribbon, as shown in Fig. 3(a). Thermal conductivity of wide ($W = 1$ μm) GNRs [Fig. 3(b)] shows a well defined minimum at $\theta_C = 0°$ (armchair direction) and a maximum occurring at $\theta_C = 30°$ (zig-zag direction). This can be attributed to the TA mode having the strongest contribution in wider ribbons, which leads to a simple, smooth variation in κ with the chiral angle. In addition, in wider ribbons with $W > \ell$, where ℓ is the phonon mean-free-path due to phonon-phonon scattering (we obtain $\ell \approx 677$ nm at room temperature, in agreement with earlier calculations[6]), phonon-phonon umklapp scattering dominates over partially diffuse boundary scattering from the rough edges, and therefore limits the angular variation in the thermal conductivity.
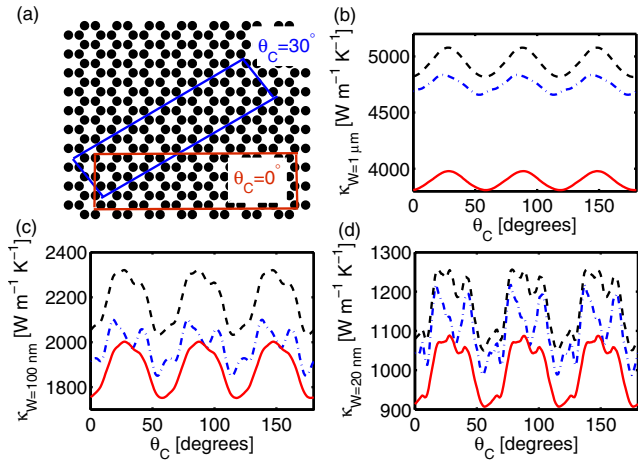
FIG. 3. (Color online) Definition of angle θ_C (a), thermal conductivity of GNRs of width 1 μm (b), 100 nm (c), and 20 nm (d) at temperatures of 100 K (blue dash-dotted curves), 200 K (black dashed curves), and 300 K (red solid curves), showing strong dependence of the thermal conductivity on the angle along which the ribbon is cut, with a minimum occurring in armchair ($\theta_C=0°$) nanoribbons, and a maximum occurring in zig-zag ($\theta_C=30°$) nanoribbons. The rms roughness of the ribbon edges was assumed to be 1 nm in all cases.

However, in narrow ribbons with $W < \ell$ [Figs. 3(c) and 3(d)], boundary scattering takes over even at room temperature (as evidenced by the strong dependence of thermal conductivity on width and edge roughness in Fig. 4(a). The contributions from LA and TA modes become roughly equal, leading to a more complex angular behavior with multiple local maxima and minima [Figs. 3(c) and 3(d)]. Nonetheless, the minimum still occurs near the armchair and the maximum near the zig-zag direction. The amount of anisotropy, given by the ratio of the thermal conductivity in the zig-zag and the armchair directions $\eta = [\kappa_{zigzag}/\kappa_{armchair} - 1]$, in-

creases with decreasing ribbon width W and increasing roughness Δ, as shown in Fig. 4(b), because of the increased influence of diffuse scattering from the rough edges.

In conclusion, we demonstrated that the physical width of the nanoribbon and the rms roughness of its line edges can be used along with angular direction as parameters to tailor the value of the thermal conductivity. Future measurements of thermal conductivity in GNRs along different chiral angles would shed more light on the thermal transport properties of GNRs and provide critical information on the relative contributions of the phonon branches to the total thermal conductivity.

[1] A. K. Geim, Science **324**, 1530 (2009).
[2] S. Ghosh, W. Bao, D. L. Nika, S. Subrina, E. P. Pokatilov, C. N. Lau, and A. A. Balandin, Nature Mater. **9**, 555 (2010).
[3] A. A. Balandin, S. Ghosh, W. Bao, I. Calizo, D. Teweldebrhan, F. Miao, and C. N. Lau, Nano Lett. **8**, 902 (2008).
[4] S. Ghosh, I. Calizo, D. Teweldebrhan, E. P. Pokatilov, D. L. Nika, A. A. Balandin, W. Bao, F. Miao, and C. N. Lau, Appl. Phys. Lett. **92**, 151911 (2008).
[5] H. Sevinçli and G. Cuniberti, Phys. Rev. B **81**, 113401 (2010).
[6] D. L. Nika, E. P. Pokatilov, A. S. Askerov, and A. A. Balandin, Phys. Rev. B **79**, 155413 (2009); S. Ghosh, D. L. Nika, E. P. Pokatilov, and A. A. Balandin, New J. Phys. **11**, 095012 (2009).
[7] J. Lan, J.-S. Wang, C. K. Gan, and S. K. Chin, Phys. Rev. B **79**, 115401 (2009); E. Muñoz, J. Lu, and B. I. Yakobson, Nano Lett. **10**, 1652 (2010); Y. Xu, X. Chen, B.-L. Gu, and W. Duan, Appl. Phys. Lett. **95**, 233116 (2009).
[8] D. L. Nika, S. Ghosh, E. P. Pokatilov, and A. A. Balandin, Appl. Phys. Lett. **94**, 203103 (2009).
[9] J. Hu, X. Ruan, and Y. P. Chen, Nano Lett. **9**, 2730 (2009); W. J. Evans, L. Hu, and P. Keblinski, Appl. Phys. Lett. **96**, 203112 (2010).
[10] A. Grüneis, R. Saito, T. Kimura, L. G. Cançado, M. A. Pimenta, A. Jorio, A. G. Souza Filho, G. Dresselhaus, and M. S. Dresselhaus, Phys. Rev. B **65**, 155405 (2002); G. G. Samsonidze, R. Saito, A. Jorio, A. G. S. Filho, A. Grüneis, M. A. Pimenta, G. Dresselhaus, and M. S. Dresselhaus, Phys. Rev. Lett. **90**, 027403 (2003).
[11] J. Maultzsch, S. Reich, C. Thomsen, H. Requardt, and P. Ordejón, Phys. Rev. Lett. **92**, 075501 (2004).
[12] R. Saito, G. Dresselhaus, and M. S. Dresselhaus, *Physical Properties of Carbon Nanotubes* (Imperial College Press, London, 1998).
[13] L. Wirtz and A. Rubio, Solid State Commun. **131**, 141 (2004).
[14] J. Zimmermann, P. Pavone, and G. Cuniberti, Phys. Rev. B **78**, 045410 (2008).
[15] J. Ziman, *Electrons and Phonons: The Theory of Transport Phenomena in Solids* (Oxford University Press, New York, 1960).
[16] Z. Aksamija and I. Knezevic, Phys. Rev. B **82**, 045319 (2010).
[17] D. T. Morelli, J. P. Heremans, and G. A. Slack, Phys. Rev. B **66**, 195304 (2002).
[18] B. D. Kong, S. Paul, M. B. Nardelli, and K. W. Kim, Phys. Rev. B **80**, 033406 (2009); P. Klemens and D. Pedraza, Carbon **32**, 735 (1994).
[19] J. X. Cao, X. H. Yan, Y. Xiao, and J. W. Ding, Phys. Rev. B **69**, 073407 (2004).
[20] G. Slack, *Solid State Physics* (Academic, New York, 1979), Vol. 34.
[21] N. Mounet and N. Marzari, Phys. Rev. B **71**, 205214 (2005).
[22] L. Wei, P. K. Kuo, R. L. Thomas, T. R. Anthony, and W. F. Banholzer, Phys. Rev. Lett. **70**, 3764 (1993).
[23] L. Lindsay, D. A. Broido, and N. Mingo, Phys. Rev. B **82**, 115427 (2010).

FIG. 4. (Color online) Dependence of the room temperature thermal conductivity of armchair GNRs (a) and anisotropy (defined as $\eta = [\kappa_{zigzag}/\kappa_{armchair} - 1]$) (b) on the GNR width. In both panels, the rms roughness Δ of the nanoribbon edges was varied from 0.1 to 1 nm in 0.1 nm steps; the direction of increasing Δ is indicated by the arrows. Thermal conductivity decreases with decreasing width W and increasing roughness Δ due to the stronger diffuse scattering with the rough edges. Anisotropy η is also larger in narrower ribbons with rougher edges due to the increasing influence of edge scattering.